CHALMERS
UNIVERSITY OF TECHNOLOGY

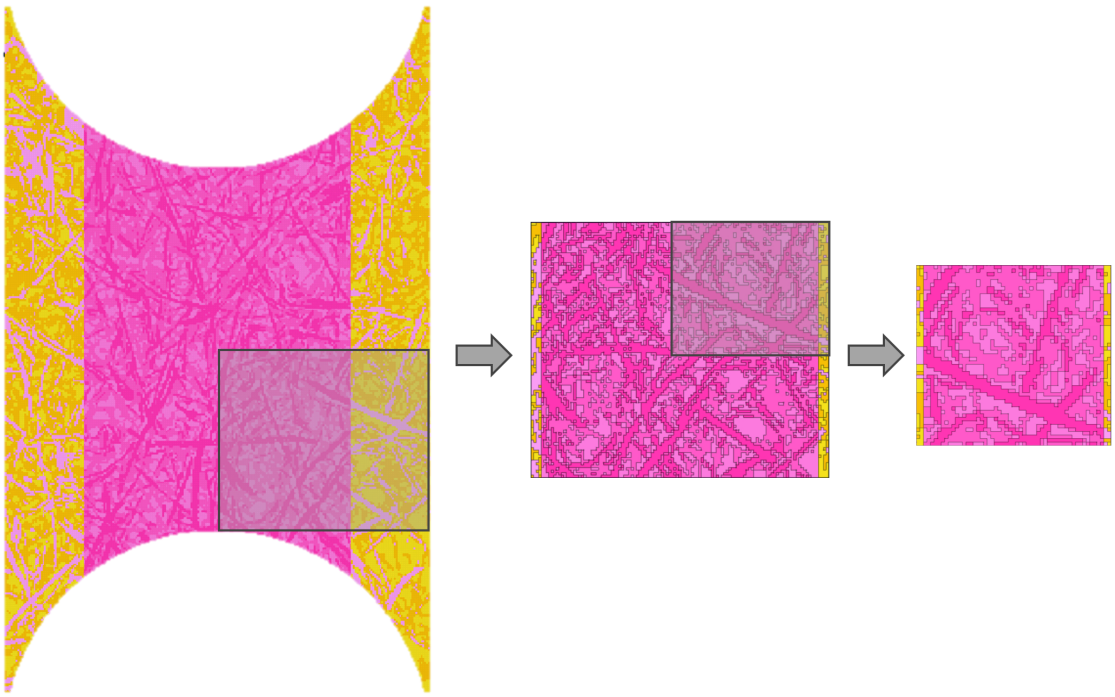

Virtual material characterization of natural fibre composites

Degree project report in Mechanical engineering

WILLIAM ABEL
VALDEMAR KULLBERG

DEPARTMENT OF INDUSTRIAL AND MATERIALS SCIENCE
CHALMERS UNIVERSITY OF TECHNOLOGY
Bachelor thesis IMSX20
Gothenburg, Sweden 2024

Degree project report IMSX20

Virtual material characterization of natural fibre composites

WILLIAM ABEL
VALDEMAR KULLBERG

CHALMERS
UNIVERSITY OF TECHNOLOGY

Department of Industrial and Materials Science
Chalmers University of Technology
In collaboration with Volvo Cars
Gothenburg, Sweden 2024

Virtual material characterization of natural fibre composites
WILLIAM ABEL
VALDEMAR KULLBERG

Supervisor: Adj. Prof. Renaud Gutkin, Volvo Cars Corporation. Department of Industrial and Materials Science, Chalmers University of Technology.
Johann Körbelin, Volvo Cars Corporation.
Examiner: Prof. Leif Asp, Department of Industrial and Materials Science.

Degree project report 2024
Department of Industrial and Materials Science
Chalmers University of Technology
SE-412 96 Gothenburg
Sweden
Telephone +46 31 772 1000

Typeset in LaTeX
Gothenburg, Sweden 2024

Virtual material characterization of natural fibre composites
William Abel
Valdemar Kullberg
Department of Industrial and Materials Science
Chalmers University of Technology

Abstract

Natural fibre composites (NFCs) are becoming common in the automotive industry due to their impressive mechanical properties and low environmental impact. The complex micro structure of NFCs makes it difficult to test the material virtually using Finite Element (FE) software. The fibre properties, such as fibre orientation and ratio, vary within the material. In 2023, a digital twin of a Kenaf/Polypropylene was developed through a master thesis at Chalmers University of Technology in cooperation with Volvo Cars AB. The FE-results from that model match the physical tensile test results. However, the process of developing a digital twin for every test specimen is expensive and time consuming.

Throughout the project, volume portions from the digital twin is generated and tested. Application of different types of boundary conditions in virtual tensile tests is made in order to find appropriate Representative Volume Elements (RVE). By finding an appropriate RVE-size, computational speed of virtual test will increase. Testing different RVEs from the same model also provides a lot of data about fibre properties.

The results shows that calculations on some RVE-sizes of NFCs are possible and provides accurate results. It also shows that fibre orientation and fibre volume fraction within the material have an impact on effective properties when running virtual tensile tests.

Keywords: Natural fibre reinforce composite, Finite Element, Representative volume elements, Virtual testing, Fibre properties, Kenaf, LS-DYNA, ANSA.

Acknowledgements

We would like to give a special thanks to Renaud Gutkin for giving us the opportunity to work on this project, while providing valuable knowledge and guidance along the way. We would also like to thank Johann Körbelin for daily support and supervision. Thank you to Emmanouil Doulgerakis and others at BETA CAE systems for supporting and answering questions related to ANSA and META, which is used in this project.

Our examiner Leif Asp has provided us with useful input and support along the project, which we are grateful for. We will also like to thank Anton Årmann and Marcus Iversen, who did a great job developing the virtual model which we are working with in this project.

Volvo Cars made this thesis possible by providing us with data, software, computers and workspace, which we are very grateful for. The CAE durability team has been very friendly and welcoming by answering questions and including us in the team, so we would like to thank them too.

Authors, Gothenburg, May 2024

List of Acronyms

Below is the list of acronyms that have been used throughout this thesis listed in alphabetical order:

CT	Computed Tomography
DDBC	Direct Displacement Boundary Condition
FE	Finite element
NFC	Natural Fibre Composite
NFRC	Natural Fibre Reinforced Composite
PP	Polypropylene
PBC	Periodic Boundary Condition
RVE	Representative Volume Element
UTBC	Uniform Traction Boundary Condition

Contents

List of Acronyms **ix**

List of Figures **xiii**

List of Tables **xv**

1 Introduction **1**
1.1 Background . . . 1
1.2 Purpose . . . 1
1.3 Goals . . . 1
1.4 Limitations . . . 1

2 Theory **3**
2.1 Natural fibre reinforced composites . . . 3
2.2 Finite element model . . . 4
2.3 Material model . . . 5
2.4 Representative Volume Elements . . . 6
2.5 Boundary conditions . . . 6
2.6 Material orientation . . . 8

3 Methods **9**
3.1 RVE definition - Regular . . . 9
3.2 RVE definition - following the crack path . . . 11
3.3 Normalization . . . 13

4 Results **15**
4.1 Effect of RVE size and material orientation . . . 15
4.2 Effect of the fibre volume fraction . . . 16
4.3 Effect of boundary conditions . . . 18
4.4 Effective properties versus RVE-size . . . 18
4.4.1 Maximum stress . . . 18
4.4.2 Young's modulus . . . 20
4.4.3 Normalized maximum stress and Young's modulus . . . 21

5 Discussion **23**
5.1 Effects of RVE size and material orientation . . . 23
5.2 Effect of fiber volume fraction . . . 23

5.3 Effect of boundary conditions 24
5.4 Effective property versus RVE-size 24

6 Conclusion **25**
6.1 Future work/Validation 25

Bibliography **27**

List of Figures

2.1 Digital twin of a Kenaf/Polypropylene test specimen. The yellow shows the no-damage model, while the pink area shows the damage model. 4
2.2 Demonstration of a RVE. 6
2.3 Visualization of the three types of boundary conditions applied on a two dimensional square. Variables: t = *traction*, u = *displacement* . . 7
2.4 Convergence of effective properties with increasing RVE size for three boundary conditions. Inspired by [5]. 8
2.5 Material orientation for the physical tests, (a) is 0°, (b) is 45°and (c) is 90°. 8

3.1 Visualization and numbering of RVEs. 9
3.2 Big cut with dimensions. Height=8.03, Length=9.37, Thickness=1.26 (mm). 10
3.3 Applied UTBC on cut 44 (1/16). Dark blue represents the fixed nodes and light blue the velocity nodes. 11
3.4 Visualization of how the RVEs along the crack is cut out. 12

4.1 Stress-strain curves for 1/16 cuts with UTBC applied. 15
4.2 Stress-strain plots for 1/4 cuts in 0° direction with UTBC applied. . . 16
4.3 Scatter plot showing maximum stress compared to fibre volume fraction for each 1/16 cut. 17
4.4 Stress-strain curves for Cut 14. 18
4.5 Maximum stress versus RVE Size. 19
4.6 Young's modulus versus RVE Size. 20
4.7 Normalized maximum stress versus RVE Size. 21
4.8 Normalized Young's modulus versus RVE Size. 22

List of Tables

2.1 Mechanical properties for some natural fibres [3]. 3

4.1 Table presenting fibre volume fraction and maximum stress for 1/16 cuts, including big cut. 16
4.2 Mean maximum stress, standard deviation of the maximum stress and median maximum stress depending on the RVE size. 19
4.3 Mean Young's modulus, standard deviation of Young's modulus and median Young's modulus depending on the RVE size. 20
4.4 Mean maximum stress, standard deviation of the maximum stress and median maximum stress depending on the RVE size, normalized. 21
4.5 Mean normalized Young's modulus, standard deviation of Young's modulus and median Young's modulus depending on the RVE size. . 22

1
Introduction

1.1 Background

In recent years, natural fibre composites (NFC) have become an interesting material choice in the automotive industry due to its material properties. They can offer a lower weight to stiffness-ratio than traditional materials such as steel or aluminum. The material consists of natural fibres from renewable plants mixed with a polymer-matrix. While physical testing of NFCs is similar to other materials, virtual testing is more challenging. Virtual testing uses software and mathematical models to replicate a physical test, for example a tensile test. This is beneficial because it is less time consuming and cheaper. Parameters such as the orientation of fibres and fibre to matrix-ratio, makes it difficult to provide accurate results from virtual tests.

A previous master thesis project [1] at Chalmers University of Technology in cooperation with Volvo Cars resulted in a digital twin of three different Kenaf/Polypropylene test specimens. Using X-ray computed Tomography of NFCs these digital models made it possible to run tensile tests using FE-software, which in comparison to physical test results turned out to be accurate.

1.2 Purpose

There is no easy method for doing virtual tests on NFCs today. If accurate results are required, a CT-scan is needed for every unique test specimen. This takes a lot of time and is expensive. This thesis investigates the possibilities of increasing the computational speed when performing a virtual test.

1.3 Goals

The goal is, based on the already existing full model, to find the smallest and most efficient reduced model to accurately represent the physical tests.

1.4 Limitations

Physical test will not be performed in this project. All data from physical tests will be provided by Volvo Cars.

All FE-calculations will be done using the previously developed virtual models, new CT-scans will not be produced.

2
Theory

2.1 Natural fibre reinforced composites

Natural fibre reinforced composites are bio-based composites that consist of natural fibres mixed with a polymer matrix. The natural fibres come from renewable plants such as hemp or other plants, which make them more sustainable than synthetic fibres. When mixed with a polymer matrix, the natural fibres are held together and protected from environmental damage. The matrix also transfers the load between the fibres. The generally low density of NFC's provides a low weight to stiffness-ratio [2]. Mechanical properties for some common natural fibres can be found in Table 2.1.

Table 2.1: Mechanical properties for some natural fibres [3].

Fibre	Density (g/cm^3)	Tensile strength (MPa)	Tensile modulus (GPa)	Elongation (%)
Jute	1.3	393-773	26.5	1.5 - 1.8
Flax	1.5	500-1500	27.6	2.7 - 3.2
Hemp	1.47	690	70	2.0 - 4.0
Kenaf	1.45	930	53	1.6

The NFC investigated in this project consist of Kenaf fibres mixed with a Polypropylene matrix. Kenaf is a commercially available and cheap plant that possess tough fibres. The kenaf plant consists of two types of fibres, bast and core. The bast fibres provide impressive mechanical properties, and can even replace glass fibres in polymer composites. There is no processing method to provide equally oriented fibres for this material. Since the fibres are biological, the length and thickness of each fibre will also vary. Another problem is that the fibre to matrix ratio will vary within the material, creating an uneven fibre distribution. Due to all these different fibre properties, the result for each test specimen will vary depending on which direction force is applied [4].

2.2 Finite element model

Prior to this project, a finite element model was developed [1]. The model is a digital twin of a Kenaf/polypropylene test specimen, more specifically the centre of the dog bone, as shown in Figure 2.1. The digital twin has the same micro structure as the physical model, and can be used in FE-software for virtual testing. Kenaf fibres, PP-matrix and air voids are modelled as solid hexahedron elements. The model has a thickness of 1.7 mm. After cleaning up the rough surfaces in ANSA, the thickness is reduced to 1.26 mm. The hexa element size is 40 μm, which results in a total of 1 926 912 hexa elements in total. To simulate tensile tests on the virtual model, boundary conditions are applied using LS-dyna. The nodes on one end is fixed in all direction, while a prescribed displacement is applied to the nodes on the other end.

(a) KE1450. Dimensions: Height=15.11, Length=9.37, Thickness=1.26 (mm)

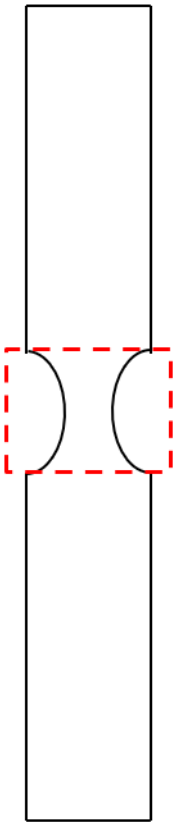

(b) The red square shows the part of the dog bone that represents the digital model.

Figure 2.1: Digital twin of a Kenaf/Polypropylene test specimen. The yellow shows the no-damage model, while the pink area shows the damage model.

2.3 Material model

The virtual model includes three different material models for fibre, matrix and void. The matrix has an elastic-plasticity model, that uses the von Mises yield criterion that assumes isotropy. This means that the material is elastic if the effective stress is lower than the yield stress. When the effective stress is equal to or higher than the yield stress, the material becomes plastic. When plasticity is achieved in the matrix, the deformation remains after unloading. The material card MAT_PIECEWISE_LINEAR_PLASTICITY is used in LS-DYNA [1].

The fibres use a brittle failure model. This means that the fibres break when the longitudinal stress or strain are too high. This failure model is strain based, and the fibre elements are deleted where the longitudinal fibre strain exceeds the ultimate fibre strain. Here, the material card MAT_ADD_EROSION is used in LS-DYNA [1].

The air voids uses an elastic material model with similar material properties as the matrix, but with a very low stiffness which has no global effect on the whole model. The reason the voids has to be modelled at all is to avoid numerical issues during virtual testing. To prevent cracks at the ends, no damage material models are applied to the elements close to the sides of the model. This will steer the crack to the center of the dog bone, which will mimic the outcome of a physical test [1].

2.4 Representative Volume Elements

If a portion of a volume can provide accurate results when compared to the full volume, that portion is a Representative Volume Element (RVE). An accurate result is obtained if the smaller portion is big enough to include sufficient microstructual features to give a statistical representation of the material. When a RVE can provide accurate results compared to the full scale model, it is very beneficial due to its increased computational speed [5]. Figure 2.2 illustrates how a RVE is made by cutting out a smaller portion of the model.

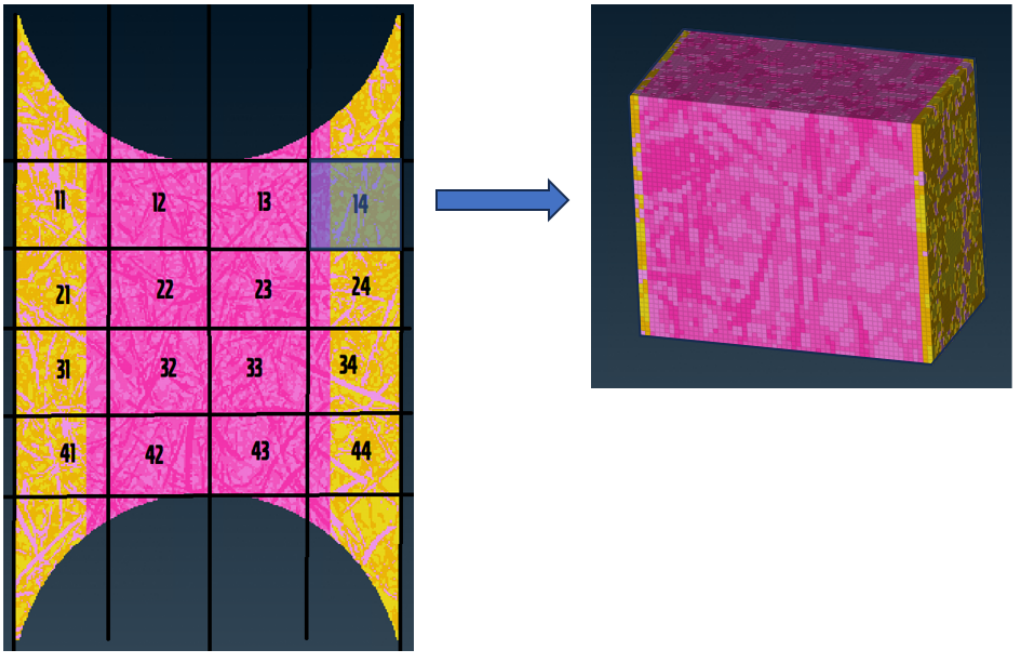

Figure 2.2: Demonstration of a RVE.

2.5 Boundary conditions

In order to determine what RVE-size is suitable for maintaining accurate results, tests with three different types of boundary conditions are compared. Uniform traction, direct displacement and periodic boundary conditions are described below, and is visualized in Figure 2.3c

- Uniform traction boundary conditions (UTBC) - When using UTBC, the fastest computational speed is achieved out of the three different types of boundary conditions. This type is what resembles the setup of a physical test the most. One end is fixed, and a traction force, t, is applied in the other end. With no other fixed ends this allows a ”waist” to form when running virtual tensile tests, like one would notice on a physical test. Figure 2.3a show the theory for UTBC [5].

- Direct displacement boundary conditions (DDBC) - Similar to UTBC, with one end fixed and applied displacement, u, on the other end. However, the four remaining sides can only move in the direction of the applied displacement. This will prevent a "waist" from forming when doing a tensile test. This type of boundary conditions decreases computational speed. Figure 2.3b show the theory for DDBC [5].

- Periodic boundary conditions (PBC) - This type will generate the most accurate results when RVE-size is decreasing. The theory is that displacement is calculated on one side of the model, and that same displacement is then applied on the opposite side. This method has the lowest computational speed out of the three different boundary conditions. Figure 2.3c show the theory for PBC [5].

As shown in Figure 2.4, the results in effective property will diverge for the three boundary conditions when RVE-size is decreasing.

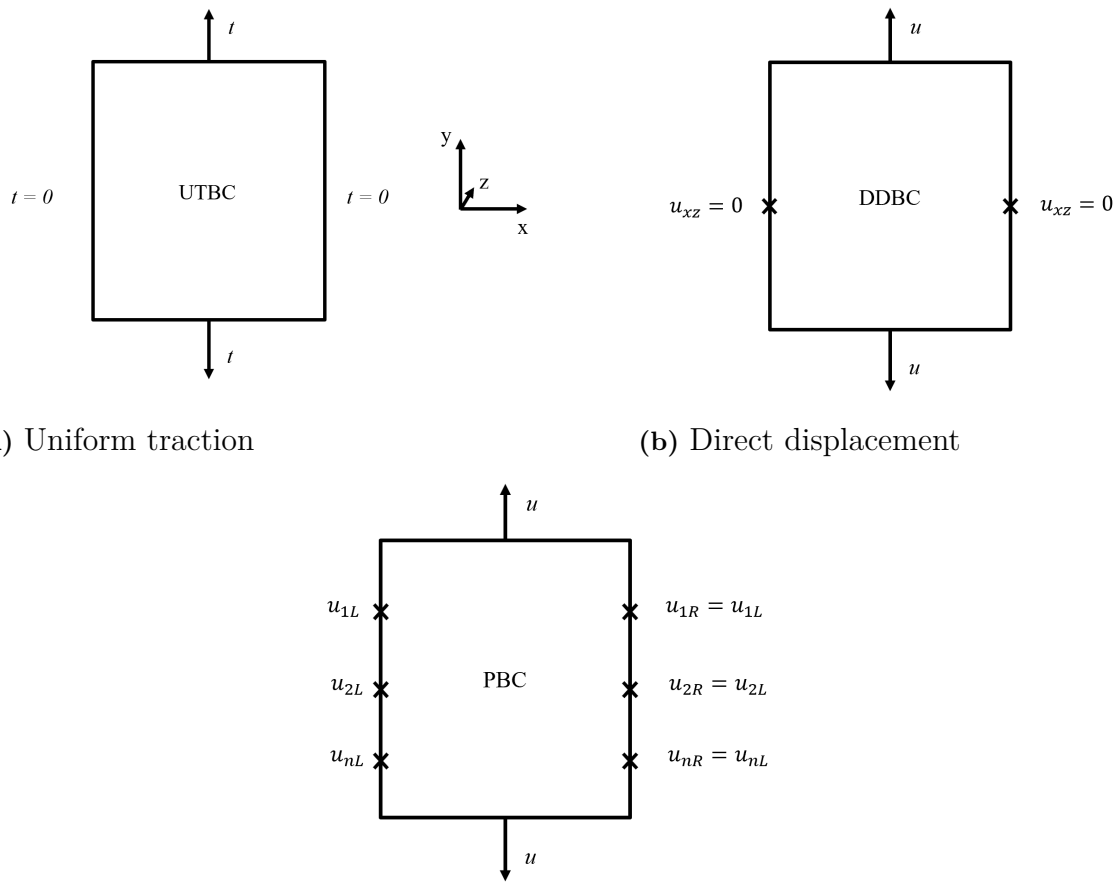

(a) Uniform traction

(b) Direct displacement

(c) Periodic

Figure 2.3: Visualization of the three types of boundary conditions applied on a two dimensional square.
Variables: t = *traction*, u = *displacement*

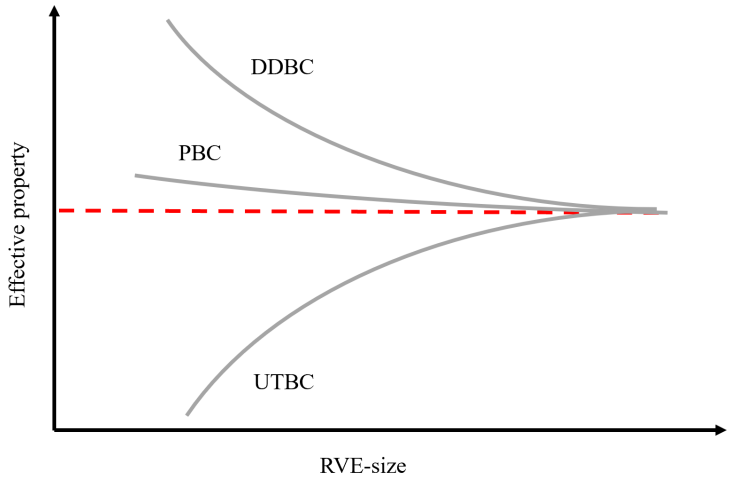

Figure 2.4: Convergence of effective properties with increasing RVE size for three boundary conditions. Inspired by [5].

2.6 Material orientation

When the NFC is manufactured the material is mixed and needled in order for the fibre and matrix to become as homogenized as possible. The mixed material is extruded from this process like a thin sheet/rug, this is the square in Figure 2.5. Test specimens in the shape of dog bones are extracted from this sheet/rug in different directions in order to capture the effect of fibre orientation in the material.

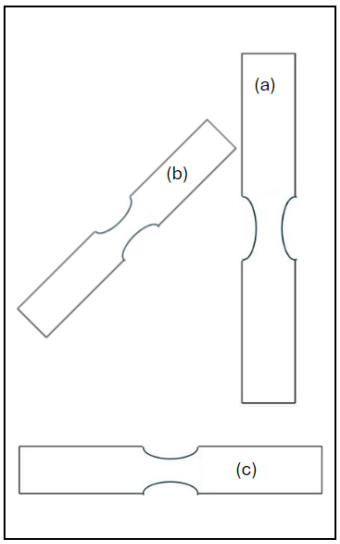

Figure 2.5: Material orientation for the physical tests, (a) is 0°, (b) is 45°and (c) is 90°.

3
Methods

3.1 RVE definition - Regular

To evaluate how the fibre volume fraction and fibre orientation affect the effective properties of the composite, cuts of the original model are made to act as RVEs. The RVEs are made in square shapes, as seen in Figure 3.1, in order to maximize the amount of samples and because the notch is too complicated to replicate in all the RVEs. In order for the results to be useful, the full sized RVE, Figure 3.1b, was also made in a square shape to eliminate the stress concentration caused by the non-linear cross-section. These cuts result in multiple unique models with a variety of fibre properties. The cutting process is done by measuring and deleting elements from the original model in ANSA.

The different cuts are numbered in a matrix-like system, followed by the size. For example "Cut 12 1/16".

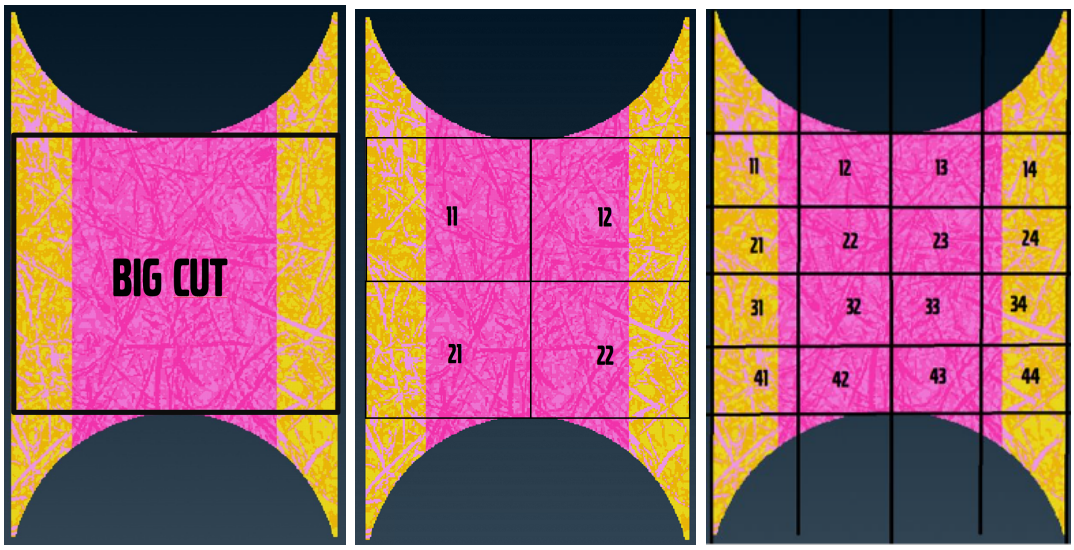

(a) Full RVE size **(b)** 1/4 RVE size. **(c)** 1/16 RVE size.

Figure 3.1: Visualization and numbering of RVEs.

Figure 3.2 shows the dimensions for the full RVE size presented in Figure 3.1a. The full sized RVE has a height of 8.03 mm and a length of 9.37 mm. RVE size 1/4 is obtained by dividing the height and length by 2. The height is therefor 4.01 mm and the length is 4.69 mm. RVE size 1/16 is obtained by dividing the length and

height from the full sized RVE by 4. This gives RVE 1/16 a height of 2.01 mm and a length of 2.34 mm. The thickness for all RVEs remains at 1.26 mm.

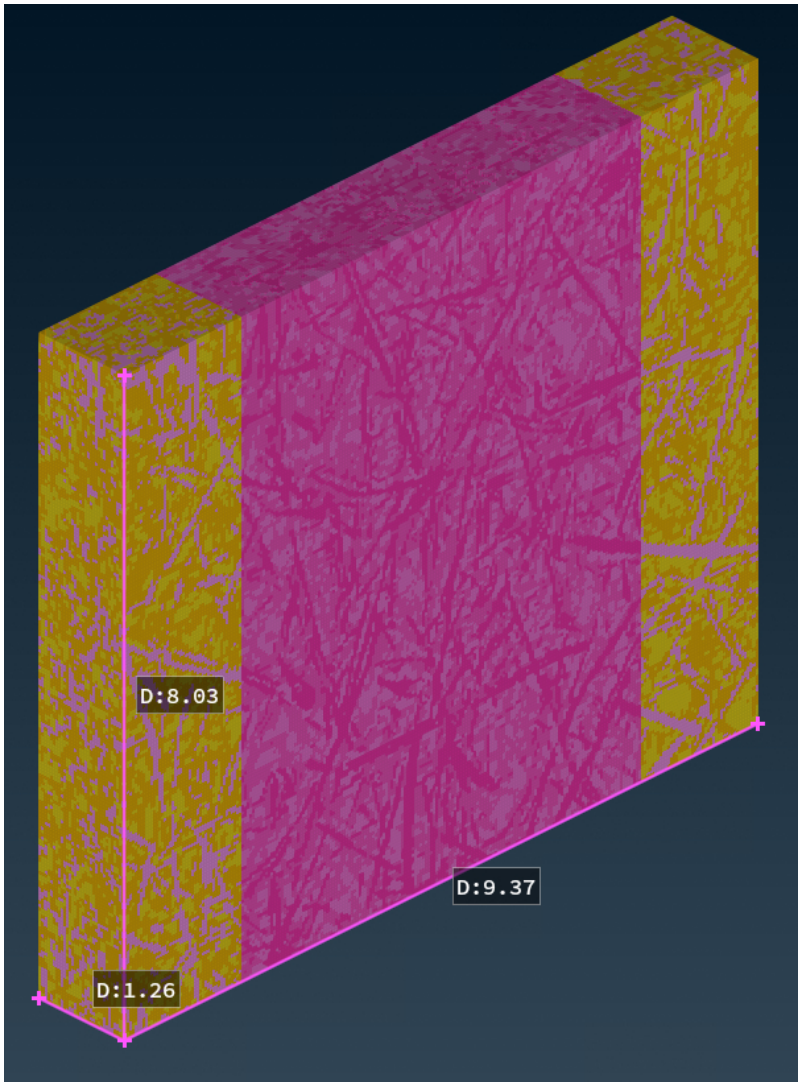

Figure 3.2: Big cut with dimensions. Height=8.03, Length=9.37, Thickness=1.26 (mm).

By dividing the height (excluding the notch) and length of the model by four, a total of 16 RVEs are obtained. The thickness remains the same (1.26 mm). In order to understand how fibre properties influence effective properties, virtual tensile tests are performed on each cut. Each cut is tested in both 0° and 90° plate direction. For these tests, uniform traction boundary conditions (UTBC) are applied. Since the aim with these tests is to study the difference in maximum stress for each piece, calculations with DDBC or PBC are deemed not necessary for these tests. Figure 3.3 shows how UTBC for these tests were applied in ANSA.

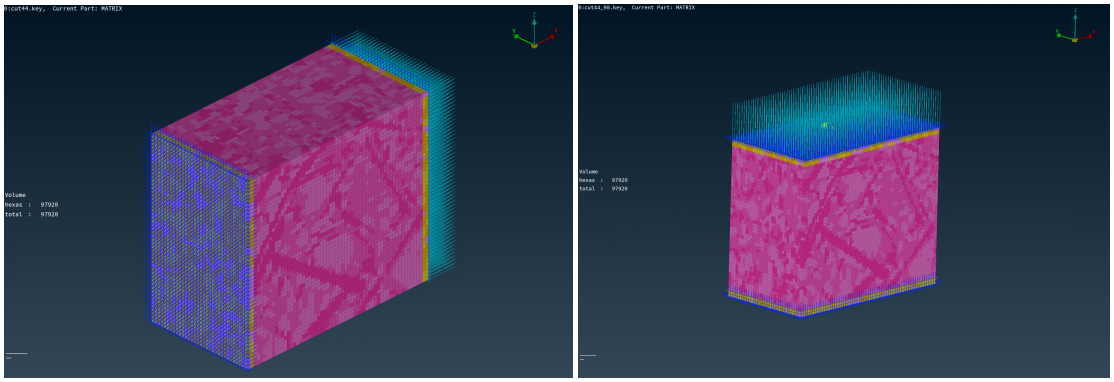

(a) Boundary conditions 0°. **(b)** Boundary conditions 90°.

Figure 3.3: Applied UTBC on cut 44 (1/16). Dark blue represents the fixed nodes and light blue the velocity nodes.

3.2 RVE definition - following the crack path

The results from the virtual tests described in 3.1 show that the cuts located near the crack of the original FE-model, present smoother stress-strain curves. Smooth curves are beneficial when running implicit FE-calculations. For this reason, cuts that follow the crack path are created. These cuts are used when comparing the different boundary conditions to RVE-size. RVEs of sizes 1/16, 1/8 and 1/4 are made along full crack path. All of which are presented in Figure 3.4, including the crack path.

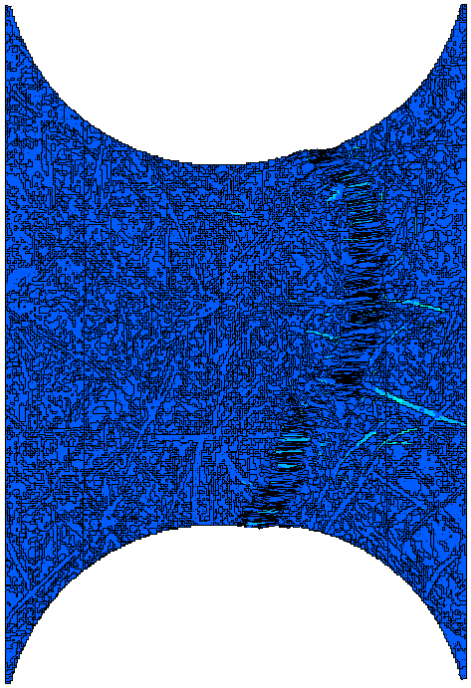

(a) Crack path formed from digital tensile test of original model.

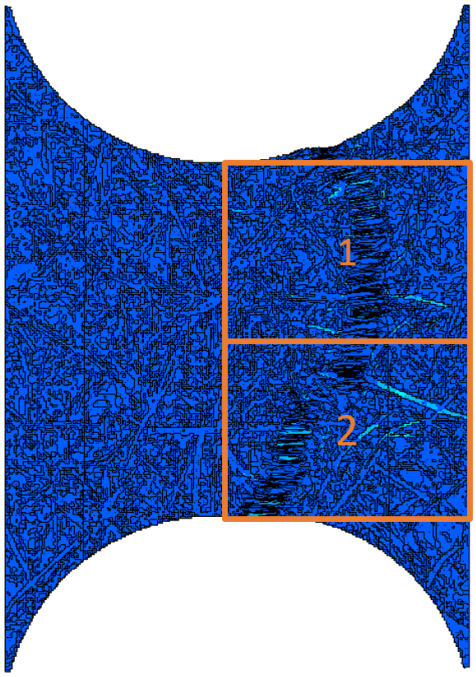

(b) 1/4 RVE-cuts following crack path. Dimensions: L=4.68, h=4.01, t=1.26 (mm).

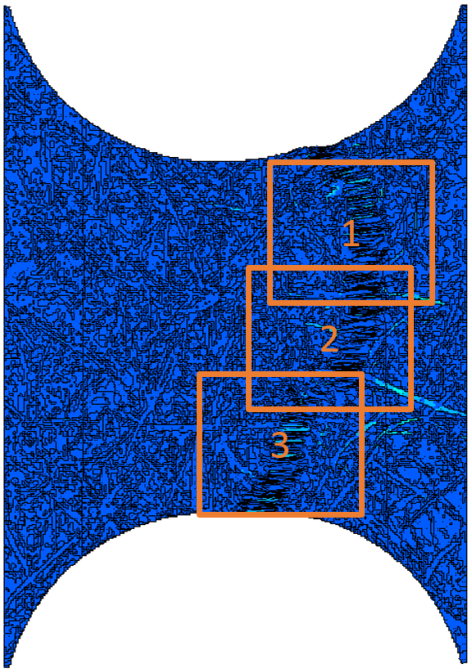

(c) 1/8 RVE-cuts following crack path. Dimension: L=3.07, h=3.07, t=1.26 (mm).

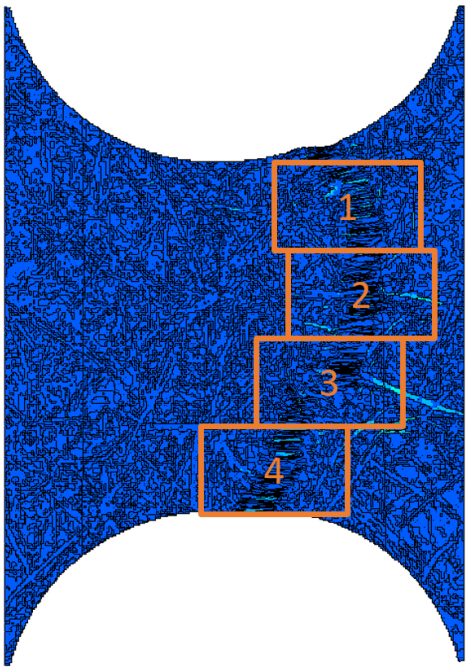

(d) 1/16 RVE-cuts following crack path. Dimensions: L=2.36, h=2.01, t=1.26 (mm).

Figure 3.4: Visualization of how the RVEs along the crack is cut out.

The idea is to create a plot that compares the effective properties for each type of boundary condition with RVE-size in a plot, and compare that plot to Figure 2.4 to see if these results follow the theory. This plot will be used to evaluate what RVE-size is suitable for testing in order to get accurate results.

3.3 Normalization

From Section 3.2 effective properties such as maximum stress and Young's modulus result. These values are normalized with its cuts fibre volume fraction. Each cut has different amount of fibre and matrix, the more fibre it has the stiffer and stronger the RVE becomes. In order to eliminate the spread of results caused by this, the normalization is made. This gives a better picture of what effect the RVE size has.

$$\frac{\textit{Effective property}}{\textit{Fibre volume fraction}} = \textit{Normalized result} \tag{3.1}$$

4
Results

4.1 Effect of RVE size and material orientation

In this section stress-strain curves for 1/16 cuts, in both 0°and 90°direction are presented. The tests are simulated with UTBC applied. The cuts included are: 12, 14, 22, 24, 32, 34, 42, 44 and big cut (see Figure 3.1).

In Figure 4.1, it shows that the stress-strain curves for each 1/16 cut differ. When comparing 0 and 90 degree direction, it also shows that the same cuts get different values for maximum stress. An interesting notice is that two groups are forming for both directions, where cuts near the crack of the original model have a lower maximum stress and smoother curves.

Note that the maximum stress is the moment the fibres break. The reason every plot continue after this point is because the matrix model does not have a damage model.

Stress-strain plots for the 1/4 cuts in the 0° direction are presented in Figure 4.2

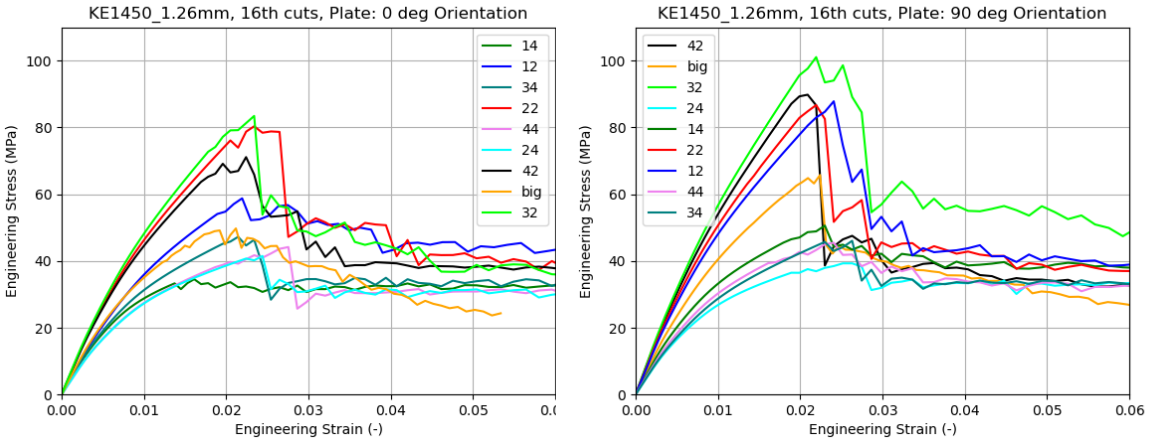

(a) 0° direction. **(b)** 90° direction.

Figure 4.1: Stress-strain curves for 1/16 cuts with UTBC applied.

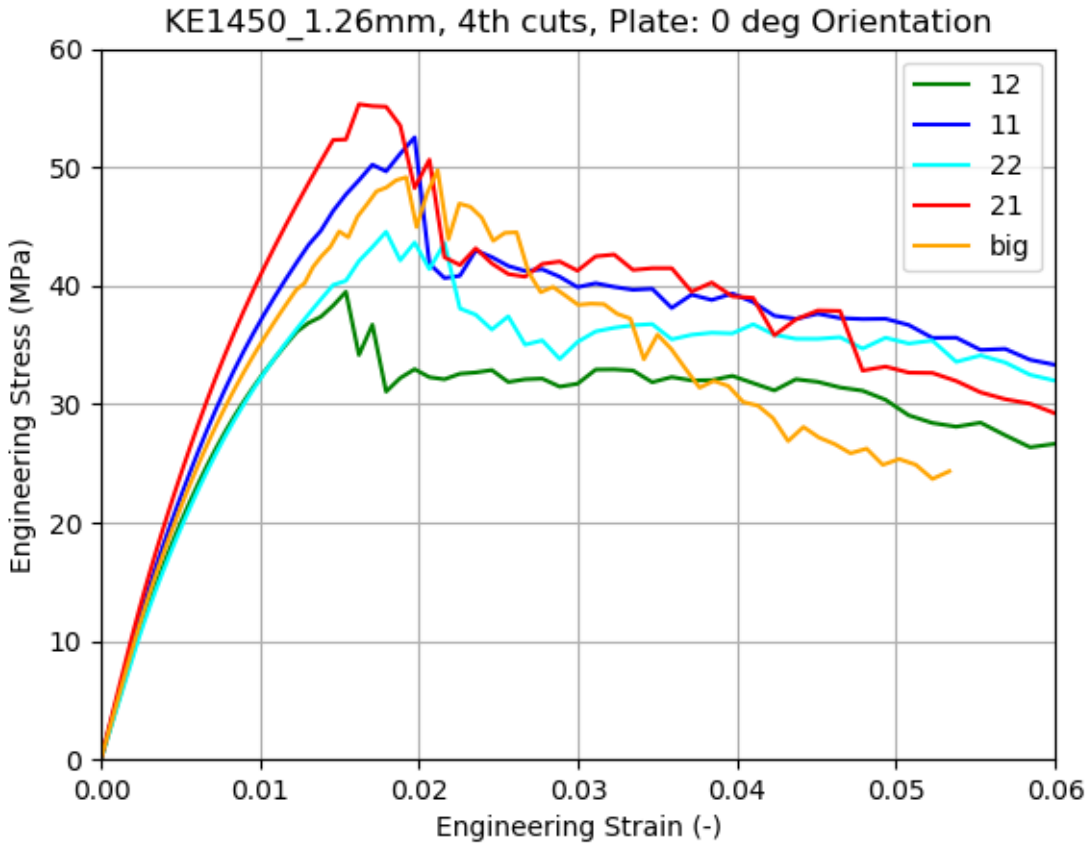

Figure 4.2: Stress-strain plots for 1/4 cuts in 0° direction with UTBC applied.

4.2 Effect of the fibre volume fraction

Table 4.1: Table presenting fibre volume fraction and maximum stress for 1/16 cuts, including big cut.

Cut #	Fibre (%)	Matrix (%)	Void (%)	Max. stress 0° (MPa)	Max. stress 90° (MPa)
12	30.8	44.5	24.7	58.8	87.8
14	21.7	54.5	23.8	34.5	50.6
22	35.0	40.3	24.8	80.3	86.7
24	18.9	53.1	28.0	41.5	39.3
32	37.6	37.4	25.0	83.4	101
34	20.2	45.0	26.5	47.2	46.0
42	35.8	38.1	26.2	71.1	90.0
44	21.0	48.9	30.2	44.2	45.5
big	28.2	45.6	26.1	49.7	65.7

Figure 4.3 shows how the maximum stress differs depending on the fibre volume fraction. Each dot represent a cut and each cut were made for 0° and 90° directions. In Table 4.1 it is noted that the the cut with the highest fibre volume fraction, cut 32, also has the highest maximum stress in both 0° and 90° direction. However, some cuts do not follow this trend. Cut 44 has a higher fibre volume fraction than cut 34, but shows a lower maximum stress in both 0° and 90° direction.

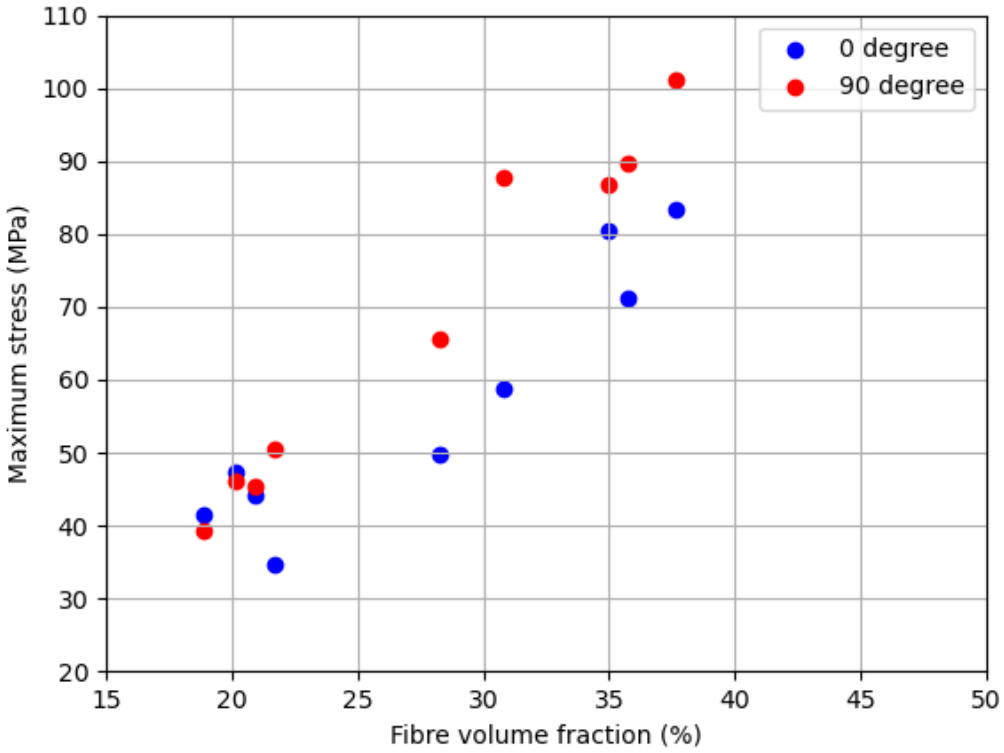

Figure 4.3: Scatter plot showing maximum stress compared to fibre volume fraction for each 1/16 cut.

4.3 Effect of boundary conditions

Figure 4.4 shows a stress/strain curve for cut 14 at 0° direction. All of the curves are identical except for the boundary conditions. Both maximum stress and Young's modulus differs even if the curves are based on the same model.

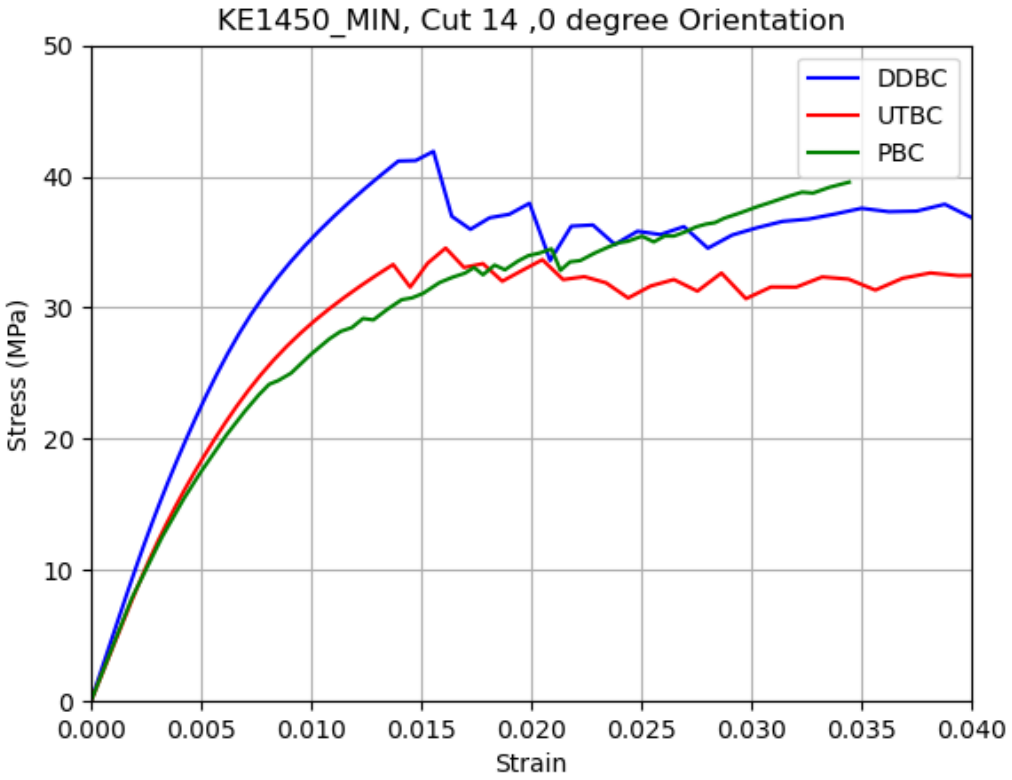

Figure 4.4: Stress-strain curves for Cut 14.

4.4 Effective properties versus RVE-size

4.4.1 Maximum stress

In Figure 4.5 the maximum stress from the virtual tensile test obtained for the different cuts are presented. These values are portrayed on the y axis. The x axis shows the RVE size. This graph is created to visualize how the maximum stress changes depending on the RVE size.

The three different types of boundary conditions are applied to the full sized virtual model. The maximum stress for them are displayed as the red area. The upper bound is set by the DDBC and the lower bound is set by the UTBC. The PBC is in between these. 11 tensile tests was obtained from Volvo. They are represented

by the grey area in the graph. This data is normalized to the full sized virtual model due to varying thickness off the test coupons. All physical test coupons have the same weight/area and had been compressed to a specific thickness. The normalization is done by scaling the maximum stress by a factor of 1.6 divided by its thickness, 1.6mm is the thickness of the virtual model.

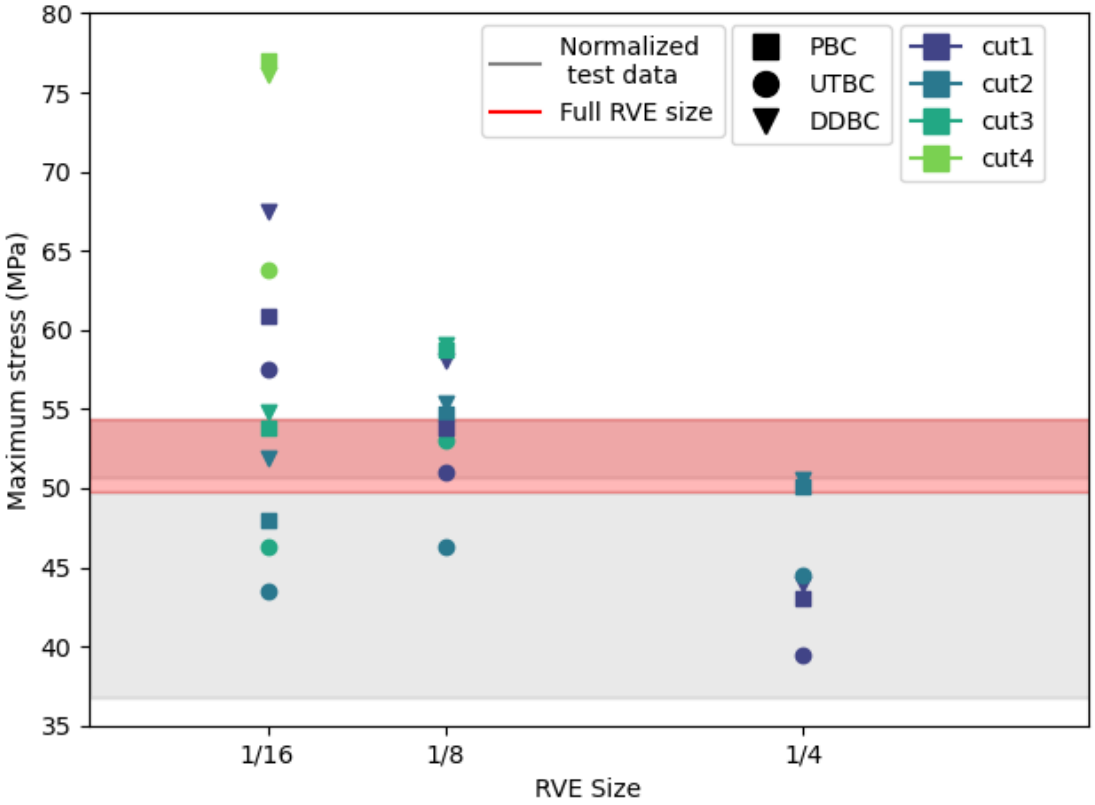

Figure 4.5: Maximum stress versus RVE Size.

As predicted in Figure 2.4, for each cut, DDBC results in the highest maximum stress, followed by the PBC and UTBC gives the lowest maximum stress.

Table 4.2 shows the mean, standard deviation and median for the maximum stress for the different RVEs. These numbers are based on the results from Figure 4.5. The percentage represents how much the results for RVE 1/8 and 1/16 increase or decrease compared to RVE size 1/4.

Table 4.2: Mean maximum stress, standard deviation of the maximum stress and median maximum stress depending on the RVE size.

RVE-size	Mean max. stress	Std. deviation max. stress	Median max. stress
1/4	45.29 | 100%	4.31 | 100%	44.25 | 100%
1/8	54.47 | 120%	4.10 | 95%	54.76 | 123%
1/16	58.43 | 129%	11.02 | 255%	56.17 | 127%

4.4.2 Young's modulus

Figure 4.6 is based on the exact same cuts and simulations as in the previous Figure 4.5 but Young's modulus is extracted and illustrated as the y-value instead of the maximum stress. Young's modulus is extracted between 0.05% and 0.25% strain from the stress/strain plot for the cuts.

Similar to Figure 4.5, the red are in the graph represents the spread of Young's modulus for the full sized model with the three different boundary conditions. The upper bound is set by the highest Young's modulus, in this case DDBC, and the lower bound is set by the lowest Young's modulus, the PBC.

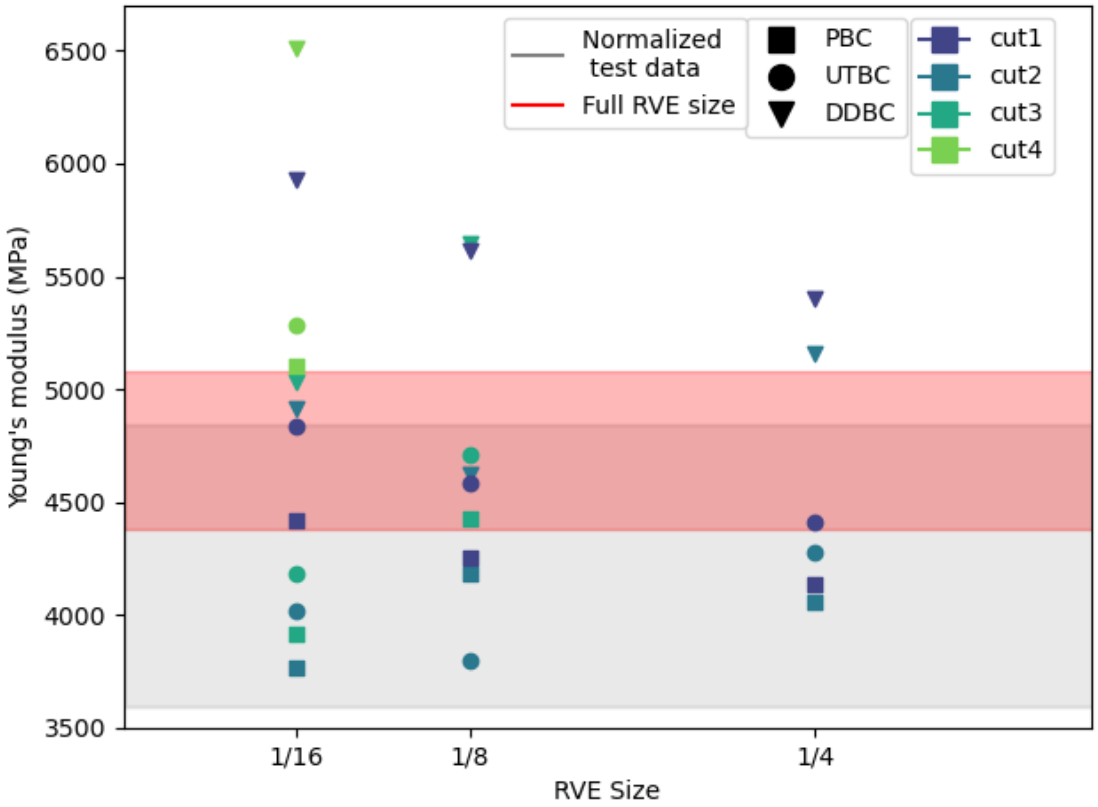

Figure 4.6: Young's modulus versus RVE Size.

Table 4.3: Mean Young's modulus, standard deviation of Young's modulus and median Young's modulus depending on the RVE size.

RVE-size	Mean Modulus	Std. deviation Modulus	Median Modulus
1/4	4.57 | 100%	0.57 | 100%	4.34 | 100%
1/8	4.65 | 102%	0.62 | 108%	4.59 | 105%
1/16	4.95 | 108%	0.94 | 165%	4.98 | 114%

4.4.3 Normalized maximum stress and Young's modulus

In Figure 4.7 normalized maximum stresses are presented. The normalized maximum stresses are the maximum stressed, previously plotted in Figure 4.5, divided by the fibre volume fraction for each cut as described in Equation 3.1.

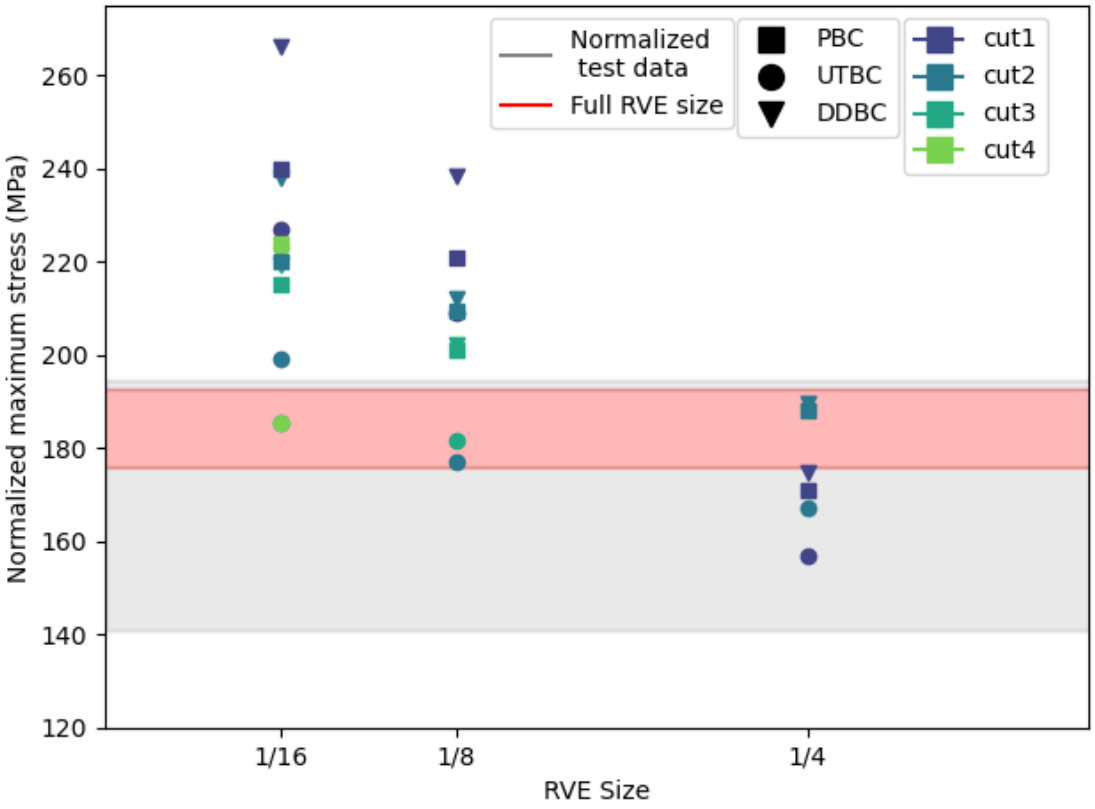

Figure 4.7: Normalized maximum stress versus RVE Size.

Table 4.4: Mean maximum stress, standard deviation of the maximum stress and median maximum stress depending on the RVE size, normalized.

RVE-size	Mean max. stress	Std. deviation max. stress	Median max. stress
1/4	174.56 | 100%	12.59 | 100%	172.83 | 100%
1/8	205.72 | 118%	18.7 | 148%	209.24 | 121%
1/16	220.15 | 126%	22.91 | 182%	220.79 | 127%

Figure 4.8 is also normalized through dividing Young's modulus by the amount of fibre.

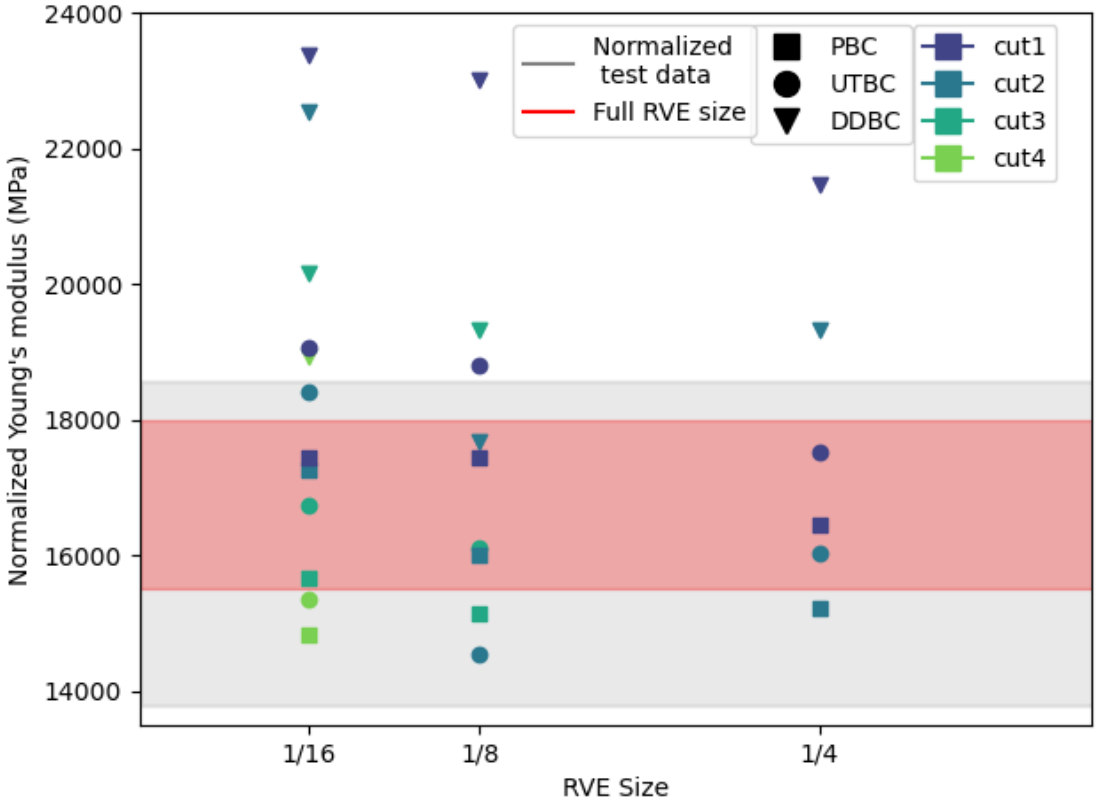

Figure 4.8: Normalized Young's modulus versus RVE Size.

Table 4.5: Mean normalized Young's modulus, standard deviation of Young's modulus and median Young's modulus depending on the RVE size.

RVE-size	Mean Modulus	Std. deviation Modulus	Median Modulus
1/4	17.67 | 100%	2.34 | 100%	16.98 | 100%
1/8	17.56 | 99%	2.60 | 111%	17.44 | 102%
1/16	18.78 | 106%	3.09 | 132%	18.18 | 107%

5
Discussion

5.1 Effects of RVE size and material orientation

In Figure 4.1, it is shown that the stress-strain curves for each 1/16 cut differ. When comparing 0° and 90° direction, it also shows that the same cuts get different values for maximum stress. It is interesting to notice that cuts near the crack of the original model have lower maximum stress and smoother curves.

The difference in maximum stress is likely related to the fibre-properties of each cut. Figure 4.3 shows that fibre volume fraction and fibre orientation have a significant effect on maximum stress for each cut. While it is difficult to measure fibre orientation in ANSA, the scatter plot still implies that orientation plays a role when it comes to the tensile strength of each cut. Properties that would be interesting to include is fibre length and cross section, but these are deemed too difficult to measure. Nevertheless, it would be interesting to see how these properties impact maximum stress.

5.2 Effect of fiber volume fraction

Due to the strong impact and the linear correlation between maximum stress and fibre volume fraction, shown in Figure 4.3, the normalization in subsection 4.4.3 was made to eliminate this factor.

One potential problem with this is that the orientation of the fibres also impact the maximum stress and Young's modulus. Examples were found where, for example, cut 34 had a higher maximum stress in both directions compared to cut 44 even though cut 44 has a higher fiber volume fraction. When these cuts are normalized according to Equation 3.1, the difference in maximum stress is increasing since the normalization does not account for fibre orientation. It is obvious that the fibre orientation in cut 34 will generate higher maximum stress than the orientation in cut 44, and the normalization to eliminate the effect of fibre amount might at the same time increase the effect caused by fibre orientation.

When looking at the results after the normalization for maximum stress, the mean maximum stress shown in Table 4.5 does not increase as much when the RVE size is lowered compared to the results for the non-normalized results shown in Table

4.2. Because of this the normalization, when done on all of the cuts together, is considered valid.

5.3 Effect of boundary conditions

When comparing graphs shown in Figure 4.5 to the theoretical graphs shown in 2.4 the different boundary conditions behave the same. DDBC has the highest maximum stress, followed by the PBC and the UTBC has the lowest. However, this relation does not occur for Young's modulus. Tests with PBC applied provide the lowest Young's modulus out of all boundary conditions. This might be a result of how the PBC is calculated in LS-DYNA and which solvers that are used.

5.4 Effective property versus RVE-size

In order for a virtual test to be useful it needs to behave like a physical test. Due to varying fibre structure in each RVE, and physical test specimen, it is logical for a spread of the effective properties to occur between same size RVEs. Hence, the spread between same sized RVEs is not the focus point. The main focus is the relation between the different boundary conditions, and how they relate to the spread in the results for the big cut. In the normalized (maximum stress/fiber volume fraction)/RVE size, shown in Figure 4.7, this occurs for the RVEs that are 1/4 of the original size. According to [5] shown in Figure 2.4 DDBC should have the highest maximum stress, followed by PBC and UTBC should have the lowest maximum stress. This behaviour occurs for the normalized maximum stress versus RVE size.

Normalized Young's modulus versus RVE size, shown in Figure 4.8, does not follow the same pattern as the maximum stress versus RVE size and the theoretical effective property versus RVE. As mentioned in 5.3 the PBC generate the lowest Young's modulus for almost every cut, which is not in line with the theory.

DDBC for all of the RVE sizes have a much higher Young's modulus than both the full sized virtual model and the physical tests, as shown in Figure 4.8. This boundary condition is therefore considered to not be representative when applied on these RVE sizes. RVE size 1/4, with PBC and UTBC, result in a similar spread compared to the full sized virtual model and is therefore considered to be a representative size.

6
Conclusion

The objective of this thesis was to identify the smallest and most efficient version of the model still representing the physical test. Based out of the results and discussion presented it is possible to make the model more efficient. A model 1/4 of the original size, applied with PBC or UTBC, is enough to represent the properties of a physical test.

6.1 Future work/Validation

A smaller RVE size could be possible. Sizes between 1/4 and 1/8 should be investigated.

The cuts for RVE 1/8 is squared compared to the cut for RVE 1/4 and 1/16 which are rectangles, the ratio between the length and the height are not identical for the different RVEs. One should consider 1/8 RVEs so the dimensions of the sides are the same.

Combine RVEs in the 0° and 90° directions in a maximum stress vs RVE size plot and find the average value, and then compare the results to the full sized RVE and physical tensile tests.

It would be interesting to test some other effective properties. Young's modulus does not seem to give accurate when PBC are applied.

Bibliography

[1] M. Iversen and A. Årmann, *Characterisation of natural fibre composites using x-ray computer tomography aided engineering*, 2023.

[2] P. Yamini, S. Rokkala, S. Rishika, P. Rani, and R. Kumar, "Mechanical properties of natural fiber reinforced composite structure," *Materials Today: Proceedings*, 2023, ISSN: 2214-7853. DOI: https://doi.org/10.1016/j.matpr.2023.04.547. [Online]. Available: https://www.sciencedirect.com/science/article/pii/S2214785323024732.

[3] R. Mahjoub, J. M. Yatim, A. R. M. Sam, and S. H. Hashemi, "Tensile properties of kenaf fiber due to various conditions of chemical fiber surface modifications," *Construction and Building Materials*, vol. 55, pp. 103–113, 2014, ISSN: 0950-0618. DOI: https://doi.org/10.1016/j.conbuildmat.2014.01.036. [Online]. Available: https://www.sciencedirect.com/science/article/pii/S0950061814000609.

[4] N. Saba, M. Paridah, and M. Jawaid, "Mechanical properties of kenaf fibre reinforced polymer composite: A review," *Construction and Building Materials*, vol. 76, pp. 87–96, 2015, ISSN: 0950-0618. DOI: https://doi.org/10.1016/j.conbuildmat.2014.11.043. [Online]. Available: https://www.sciencedirect.com/science/article/pii/S0950061814012628.

[5] D. J. Walters, D. J. Luscher, and J. D. Yeager, "Considering computational speed vs. accuracy: Choosing appropriate mesoscale rve boundary conditions," *Computer Methods in Applied Mechanics and Engineering*, vol. 374, p. 113 572, 2021, ISSN: 0045-7825. DOI: https://doi.org/10.1016/j.cma.2020.113572. [Online]. Available: https://www.sciencedirect.com/science/article/pii/S004578252030757X.

DEPARTMENT OF SOME SUBJECT OR TECHNOLOGY
CHALMERS UNIVERSITY OF TECHNOLOGY
Gothenburg, Sweden
www.chalmers.se

CHALMERS
UNIVERSITY OF TECHNOLOGY